Inorganic Chemistry
Article

Inorg. Chem. **2009**, *48*, 8703–8708 **8703**
DOI: 10.1021/ic9006444

Glycine-Templated Manganese Sulfate with New Topology and Canted Antiferromagnetism

Zhehui Weng,[†,‡] Zilu Chen,[†] and Fupei Liang*[,†]

[†]*College of Chemistry and Chemical Engineering, Guangxi Normal University, Guilin 541004, People's Republic of China, and* [‡]*State Key Laboratory of Coordination Chemistry, Coordination Chemistry Institute, School of Chemistry and Chemical Engineering, Nanjing University, Nanjing 210093, China*

Received April 2, 2009

A new glycine-templated manganese(II) sulfate, $(C_2NO_2H_5)MnSO_4$ (**1**), has been solvothermally synthesized and characterized crystallographically and magnetically. Crystal data for **1**: monoclinic, space group $P2_1/m$, $a = 4.8884(10)$ Å, $b = 7.8676(14)$ Å, $c = 8.0252(15)$ Å, $\beta = 106.524(2)°$, $V = 295.90(10)$ Å^3, $Z = 2$. The glycine bridges Mn^{II} ions in μ_2 mode and sulfate in η^3,μ^4 mode. Along the *b* direction, the neighboring Mn^{II} ions were bridged to each other by two sulfate ions and one glycine ligand to form a triple-stranded braid. The adjacent braids were connected via the sulfate ions to give a two-dimensional framework with a novel binodal 4,6-connected $(3^2;4^2;5^2)(3^4;4^4;5^4;6^3)$ topology. The compound exhibits a spin-canted antiferromagnetic behavior with a weak ferromagnetic transition below 9 K, and the estimated canting angle is 0.13°.

Introduction

More and more attention has been paid to the design and synthesis of novel inorganic open frameworks over the past decades because of their variety of intriguing structural topologies[1] and their potential applications as microporous,[2] magnetic,[3] nonlinear-optical, and fluorescent[4] materials. Generally, the metallic cation and oxo anion are the two parts that make up the inorganic skeleton of such materials. Up to now, most of the reported open-framework materials are metal phosphates and phosphites.[5] Recently, sulfate-based open-framework compounds have started to flourish since Rao et al. reported the first two one-dimensional (1D) cadmium sulfates,[6] and many open-framework materials of metal sulfates, including organic-template-directing uranium sulfates,[7] lanthanum sulfates,[8] and others,[9] have been extensively studied. In this context, most of the reported

*To whom correspondence should be addressed. E-mail: fliangoffice@yahoo.com. Tel: 86-773-5846771. Fax: 86-773-5832294.

(1) (a) Moulton, B.; Zaworotko, M. J. *Chem. Rev.* **2001**, *101*, 1629–1658. (b) Sun, Y.-Q.; Yang, G.-Y. *Dalton Trans.* **2007**, 3771–3781.

(2) (a) Kuznicki, S. M.; Bell, V. A.; Nair, S.; Hillhouse, H. W.; Jacubinas, R. M.; Braunbarth, C. M.; Toby, B. H.; Tsapatsis, M. *Nature* **2001**, *412*, 720–724. (b) Yaghi, O. M.; Li, H.; Davis, C.; Richardson, D.; Groy, T. L. *Acc. Chem. Res.* **1998**, *31*, 474–484. (c) Eddaoudi, M.; Moler, D. B.; Li, H.; Chen, B.; Reineke, T. M.; O'Keeffe, M.; Yaghi, O. M. *Acc. Chem. Res.* **2001**, *34*, 319–330.

(3) Zheng, Y.-Z.; Xue, W.; Tong, M.-L.; Chen, X.-M.; Grandjean, F.; Long, G. J. *Inorg. Chem.* **2008**, *47*, 4077–4087.

(4) (a) Serre, C.; Pelle, F.; Gardant, N.; Ferey, G. *Chem. Mater.* **2004**, *16*, 1177–1182. (b) Hartmann-Thompson, C.; Keeley, D. L.; Pollock, K. M.; Dvornic, P. R.; Keinath, S. E.; Dantus, M.; Gunaratne, T. C.; LeCaptain, D. J. *Chem. Mater.* **2008**, *20*, 2829–2838.

(5) (a) Murugavel, R.; Choudhury, A.; Walawalkar, M. G.; Pothiraja, R.; Rao, C. N. R. *Chem. Rev.* **2008**, *108*, 3549–3655. (b) Cheetham, A. K.; Férey, G.; Loiseau, T. *Angew. Chem., Int. Ed.* **1999**, *38*, 3268–3292. (c) Rodgers, J. A.; Harrison, W. T. A. *Chem. Commun.* **2000**, 2385–2386. (d) Sassoye, C.; Loiseau, T.; Férey, G.; Taulelle, F. *Chem. Commun.* **2000**, 943–944. (e) Liu, Y.; Du, H.; Xiao, F.-S.; Zhu, G.; Pang, W. *Chem. Mater.* **2000**, *12*, 665–670. (f) Choudhury, A.; Natarajan, S.; Rao, C. N. R. *Inorg. Chem.* **2000**, *39*, 4295–4304. (g) Zhu, J.; Bu, X.; Feng, P.; Stucky, G. D. *J. Am. Chem. Soc.* **2000**, *122*, 11563–11564. (h) Fernández, S.; Mesa, J. L.; Pizarro, J. L.; Lezama, L.; Arriortua, M. I.; Teófilo, R. *Angew. Chem., Int. Ed.* **2002**, *41*, 3683–3685. (i) Riou, D.; Fayon, F.; Massiot, D. *Chem. Mater.* **2002**, *14*, 2416–2420.

(6) (a) Behera, J. N.; Gopalkrishnan, K. V.; Rao, C. N. R. *Inorg. Chem.* **2004**, *43*, 2636–2642. (b) Rao, C. N. R.; Behera, J. N.; Dan, M. *Chem. Soc. Rev.* **2006**, *35*, 375–387. (c) Behera, J. N.; Rao, C. N. R. *Inorg. Chem.* **2006**, *45*, 9475–9479. (d) Behera, J. N.; Rao, C. N. R. *J. Am. Chem. Soc.* **2006**, *128*, 9334–9335.

(7) (a) Doran, M.; Norquist, A. J.; O'Hare, D. *Chem. Commun.* **2002**, 2946–2947. (b) Norquist, A. J.; Doran, M. B.; Thomas, P. M.; O'Hare, D. *Inorg. Chem.* **2003**, *42*, 5949–5953. (c) Norquist, A. J.; Thomas, P. M.; Doran, M. B.; O'Hare, D. *Chem. Mater.* **2002**, *14*, 5179–5184. (d) Halasyamani, P. S.; Walker, S. M.; O'Hare, D. *J. Am. Chem. Soc.* **1999**, *121*, 7415–7416. (e) Norquist, A. J.; Doran, M. B.; Thomas, P. M.; O'Hare, D. *Dalton Trans.* **2003**, 1168–1175. (f) Doran, M. B.; Cockbain, B. E.; Norquist, A. J.; O'Hare, D. *Dalton Trans.* **2004**, 3810–3814. (g) Thomas, P. M.; Norquist, A. J.; Doran, M. B.; O'Hare, D. *J. Mater. Chem.* **2003**, *13*, 88–92. (h) Doran, M. B.; Norquist, A. J.; O'Hare, D. *Inorg. Chem.* **2003**, *42*, 6989–6995.

(8) (a) Xing, Y.; Shi, Z.; Li, G.; Pang, W. *Dalton Trans.* **2003**, 940–943. (b) Xing, Y.; Liu, Y.; Shi, Z.; Meng, H.; Pang, W. *J. Solid State Chem.* **2003**, *174*, 381–385. (c) Dan, M.; Behera, J. N.; Rao, C. N. R. *J. Mater. Chem.* **2004**, *14*, 1257–1265. (d) Bataille, T.; Louër, D. *J. Solid State Chem.* **2004**, *177*, 1235–1243.

(9) (a) Lin, J.; Guo, D.-W.; Tian, Y.-Q. *Cryst. Growth Des.* **2008**, *8*, 4571–4575. (b) Behera, J. N.; Rao, C. N. R. *Chem. Asian J.* **2006**, *1*, 742–750. (c) Zhu, Y.; Zhou, G.; Xu, Y.; Zhu, D.; Zheng, X. *Z. Anorg. Allg. Chem.* **2008**, *634*, 545–548. (d) Zhou, W.; Chen, Q.; Zhu, D.; Xu, Y. *Z. Anorg. Allg. Chem.* **2009**, *635*, 572–576. (e) Behera, J. N.; Paul, G.; Choudhury, A.; Rao, C. N. R. *Chem. Commun.* **2004**, 456–457. (f) Telfer, S. G.; Kuroda, R.; Lefebvre, J.; Leznoff, D. B. *Inorg. Chem.* **2006**, *45*, 4592–4601. (g) Niu, Y.; Li, Z.; Song, Y.; Tang, M.; Wu, B.; Xin, X. *J. Solid State Chem.* **2006**, *179*, 4003–4010.

Published on Web 08/21/2009

sulfate-based materials were synthesized using organic amines as templates.[6c,7a,7f,9b−9d] No transition-metal sulfate of open framework templated by a amino acid molecule has ever been reported, although some 1D and two-dimensional (2D) phosphate or phosphite open-framework structure materials with amino acids as templates, such as a L-asparagine molecule templated 1D zinc phosphate,[10] a histidine-templated 1D ladder zinc phosphate,[11] a histidine-controlled 2D zinc phosphate,[12] a DL-histidine-templated 2D-layered zinc phosphate,[13] a glycine-templated 2D-layered gallophosphate,[14] have been documented. Open frameworks developed by using amino acids as templates may allow for the generation of novel materials with unique structures because of the zwitterionic characteristics and coordination ability of the template molecules. On the other hand, research on the properties of the sulfated open-framework materials has revealed interesting magnetic properties for some systems,[6d,9e,15] such as the strong ferromagnetic coupling between the vanadium ions of a vanadium(III) compound,[15a] the strong antiferromagnetic interactions between cobalt ions and magnetic frustration of a cobalt(II) sulfate,[9e] the long-range magnetic ordering and ferrimagnetic ordering of the iron sulfates,[15b,d,e] and the canted antiferromagnetism of a nickel(II) compound.[6d] All of above-mentioned interesting metal sulfate materials have Kagome structures with a corner-sharing triangular lattice. Relatively fewer studies were carried out on the magnetic properties of the metal sulfate open framework with no Kagome structure.[16] In view of the above observation, we intended to study the synthesis and magnetic properties of the amino acid templated transition-metal sulfate. Fortunately, a novel glycine-templated 2D manganese(II) sulfate hybrid material, $(C_2NO_2H_5)MnSO_4$ (**1**), was successfully obtained. To the best of our knowledge, this is the first example of an amino acid templated transition-metal sulfate material with an extended network structure. The magnetic investigations reveal that the compound displays interesting spin-canting antiferromagnetism below 9 K, and the structure studies show that it features a 4,6-connected framework with novel $(3^2;4^2;5^2)(3^4;4^4;5^4;6^3)$ topology that has never been reported before.

Experimental Section

Materials and Physical Measurements. Commercially available solvents and chemicals were used without further purification. IR spectra were recorded in the range 400−4000 cm^{-1} on a Perkin-Elmer PE Spectrum One FTIR spectrometer using a KBr pellet. Elemental analyses (C, H, and N) were performed on a Perkin-Elmer PE 2400 II CHN elemental analyzer. Powder X-ray diffraction (PXRD) intensities were measured at 298 K on a Rigaku D/max-IIIA diffractometer (Cu Kα, λ = 1.540 56 Å). The magnetic susceptibility measurements were carried out on polycrystalline samples using a Quantum Design MPMS-XL-5 SQUID magnetometer in the temperature range 2−300 K and a magnetic field up to 5 T. Diamagnetic corrections were estimated from Pascal's constants.

Preparation of $(C_2NO_2H_5)MnSO_4$ (1). $MnSO_4 \cdot H_2O$ (0.1699 g, 1 mmol), glycine (0.038 g, 0.5 mmol), and 1,2,4-triazole (trz; 0.0698 g, 1 mmol) were dissolved in a mixed solvent of CH_3CH_2OH (5 mL), CH_3CN (3 mL), and H_2O (7 mL). The pH value was then adjusted to 6.5 with triethylamine. A white precipitate was formed after stirring. The resulting mixture was transferred and sealed in a 25-mL Teflon-lined stainless steel vessel, which was heated at 130 °C for 6 days and subsequently cooled slowly to room temperature. The product was filtered off and washed with EtOH and water, and the colorless block-shaped crystals were collected and dried in air (0.150 g, 66% in yield). Anal. Calcd for $MnC_2H_5SNO_6$: C, 10.62; H, 2.23; N, 6.20. Found: C, 10.11; H, 2.49; N, 6.85. IR (KBr pellet, cm^{-1}): 3156s, 1632s, 1610s, 1474s, 1421s, 1353s, 1166vs, 1114vs, 1080vs, 1043vs, 990s, 902s, 650w, 606s.

X-ray Crystallography. Diffraction intensity data were collected at room temperature on a Bruker CCD area detector with graphite-monochromated Mo Kα radiation (λ = 0.710 73 Å). An empirical absorption correction was applied using the *SADABS* program.[17] The structure were solved by direct methods and refined using full-matrix least squares based on F^2 with all non-hydrogen atoms anisotropic and hydrogen atoms included on calculated positions, riding on their carriers. All calculations were done with the *SHELXS-97* and *SHELXL-97* program packages.[18] Detailed information about the crystal data and structure determination is summarized in Table 1, and the selected bond distances and angles are given in Table 2.

Results and Discussion

Synthesis and Characterization. Complex **1** was prepared by the reaction of $MnSO_4 \cdot H_2O$, trz, and glycine in a mixed solvent of CH_3CH_2OH, CH_3CN, and H_2O under solvothermal conditions. The reaction at 130 °C for 6 days produced colorless block-shaped crystals in 66% yield. The phase purity of the compound was confirmed by its experimental PXRD, which is identical with the simulated one (Figure S1 in the Supporting Information). It is noteworthy that the reagent of trz is not involved in coordination to Mn^{II}, but it is rather important in the formation of compound **1**. Similar reactions in the absence of trz or in the presence of other bases failed to afford the compound, indicating that the formation of compound **1** is mainly induced by the uncommon base of trz.

The IR spectrum of complex **1** (Figure S2 in the Supporting Information) shows characteristic IR bands of sulfate ions, with the IR-active region for the SO_4 tetrahedron located at 1114 and 606 cm^{-1}. As we know, the IR spectrum of the free ionic sulfate consists of two bands at 1105 and 615 cm^{-1}, assigned to the $\nu_3(F_2)$

(10) Gordon, L. E.; Harrison, W. T. A. *Inorg. Chem.* **2004**, *43*, 1808–1809.
(11) Fan, J.; Slebodnick, C.; Angel, R.; Hanson, B. E. *Inorg. Chem.* **2005**, *44*, 552–558.
(12) Chen, L.; Bu, X. *Chem. Mater.* **2006**, *18*, 1857–1860.
(13) Zhao, L.; Li, J.; Chen, P.; Dong, Z.; Yu, J.; Xu, R. *CrystEngComm* **2008**, *10*, 497–501.
(14) Hasnaoui, M. A.; Simon-Masseron, A.; Gramlich, V.; Patarin, J.; Benguedach, A. *Eur. J. Inorg. Chem.* **2005**, 536–542.
(15) (a) Grohol, D.; Papoutsakis, D.; Nocera, D. G. *Angew. Chem., Int. Ed.* **2001**, *40*, 1519–1521. (b) Paul, G.; Choudhury, A.; Rao, C. N. R. *Chem. Commun.* **2002**, 1904–1905. (c) Grohol, D.; Nocera, D. G. *J. Am. Chem. Soc.* **2002**, *124*, 2640–2646. (d) Rao, C. N. R.; Sampathkumaran, E. V.; Nagarajan, R.; Paul, G.; Behera, J. N.; Choudhury, A. *Chem. Mater.* **2004**, *16*, 1441–1446. (e) Bartlett, B. M.; Nocera, D. G. *J. Am. Chem. Soc.* **2005**, *127*, 8985–8993. (f) Shores, M. P.; Nytko, E. A.; Bartlett, B. M.; Nocera, D. G. *J. Am. Chem. Soc.* **2005**, *127*, 13462–13463. (g) Pati, S. K.; Rao, C. N. R. *Chem. Commun.* **2008**, 4683–4693. (h) J. N. Behera, C. N. R. R. *Dalton Trans.* **2007**, 669–673.
(16) (a) Xu, L.; Wang, E.; Peng, J.; Huang, R. *Inorg. Chem. Commun.* **2003**, *6*, 740–743. (b) Shatruk, M.; Chouai, A.; Prosvirin, A. V.; Dunbar, K. R. *Dalton Trans.* **2005**, 1897–1902. (c) Yuan, Y.-P.; Wang, R.-Y.; Kong, D.-Y.; Mao, J.-G.; Clearfield, A. *J. Solid State Chem.* **2005**, *178*, 2030–2035. (d) Li, G.; Xing, Y.; Song, S.; Xu, N.; Liu, X.; Su, Z. *J. Solid State Chem.* **2008**, *181*, 2406–2411.
(17) Sheldrick, G. M. *SADABS, Siemens Area Detector Absorption Correction Program*; University of Göttingen: Göttingen, Germany, 1994.
(18) (a) Sheldrick, G. M. *SHELXL-97, Program for Crystal Structure Refinement*; University of Göttingen: Göttingen, Germany, 1997. (b) Sheldrick, G. M. *SHELXS-97, Program for Crystal Structure Solution*; University of Göttingen: Göttingen, Germany, 1997.

Table 1. Crystallographic Data and Structure Refinement Results for Compound **1**

empirical formula	$C_2H_5MnNO_6S$
fw	226.07
cryst syst	monoclinic
space group	$P2_1/m$
a (Å)	4.8884(10)
b (Å)	7.8676(14)
c (Å)	8.0252(15)
β (deg)	106.524(2)
V (Å^3)	295.90(10)
Z	2
ρ_{calcd} (g cm^{-3})	2.537
μ (mm^{-1})	2.563
R_{int}	0.0244
R_1 [$I > 2\sigma(I)$]	0.0832
wR_2 (all data)	0.1843
GOF on F^2	1.173
$\Delta\rho_{max}$, $\Delta\rho_{min}$ (e Å^{-3})	1.805, −2.5

Table 2. Selected Bond Lengths (Å) and Angles (deg) of Compound **1**[a]

Mn1−O1	2.123(8)	Mn1−O3	2.131(7)
Mn1−O2	2.353(6)		
O1−Mn1−O1A	180.000(1)	O3C−Mn1−O2A	90.9(3)
O1−Mn1−O3C	93.5(3)	O3B−Mn1−O2A	89.1(3)
O1A−Mn1−O3C	86.5(3)	O1−Mn1−O2	90.0(3)
O1−Mn1−O3B	86.5(3)	O1A−Mn1−O2	90.0(3)
O1A−Mn1−O3B	93.5(3)	O3C−Mn1−O2	89.1(3)
O3C−Mn1−O3B	180.000(1)	O3B−Mn1−O2	90.9(3)
O1−Mn1−O2A	90.0(3)	O2A−Mn1−O2	180.0(5)
O1A−Mn1−O2A	90.0(3)		

[a] Symmetry codes: A, $-x$, $-y$, $1-z$; B, $-1-x$, $-y$, $1-z$; C, $1+x$, y, z.

stretching [ν_d(SO)] and $\nu_4(F_2)$ stretching [δ_d(OSO)] modes, respectively.[19] The coordination of SO_4^{2-} to metal ions decreases the symmetry of the group, and the ν_3 and ν_4 modes are then split. In our case, the SO_4^{2-}-site symmetry is lowered by bridging coordination; thus, the IR bands at 1114 cm^{-1} and the shoulders at 1166, 1080, and 1043 cm^{-1} are rationally attributed to the ν_3 modes, and the bands/shoulders at 650, 606, and 532 cm^{-1} are assigned to the ν_4 modes. The bands at the 1632−1353 cm^{-1} region are assigned to ν_{as}(−COO) and ν_s(−COO) modes, and the band at 3156 cm^{-1} is for $\nu(NH_3^+)$.

Thermogravimetric analysis (TGA) of **1** was performed on powder samples at a heating rate of 10 °C min^{-1} under flowing nitrogen (15 mL min^{-1}). The TGA curve (Figure S3 in the Supporting Information) shows no obvious weight loss until 300 °C, indicating the good thermal stability of the compound. **1** decomposes in a two-step manner. The first weight loss corresponds to the pyrolysis of glycine and sulfate in the range 300−400 °C (obsd 48.7%; calcd 49.2%). The second weight loss occurs in the range 530−710 °C (obsd 22.1%; calcd 19.5%). The final residue is manganese oxide. The remaining weight of 29.2% is close to the calculated value of 31.4%.

Crystal Structure. Compound **1** crystallizes in the $P2_1/m$ space group. The structure of **1** consists of 1D Mn^{II}−amino acid−acetic acid chains connected by sulfate ions. Each Mn^{II} is coordinated in a centrosymmetric and axially elongated octahedral environment with two sulfate ions in the axial positions [Mn−O 2.353(6) Å], two oxygen atoms from two sulfate groups, and two μ_2-bridged carboxylate groups in the basal plane [Mn−O 2.131(7) and 2.123(8) Å], as depicted in Figure 1a. The bond angles around the manganese center range from 86.5(3)° to 93.5(3)°. The carboxyl group of glycine coordinates to Mn^{II} ions in a μ_2 mode. The amino group is free from coordination and is disordered. The sulfate ion in the structure binds four Mn^{II} ions in a η^3,μ^4-coordination mode. Every two neighboring Mn^{II} ions along the b axis are connected by one carboxylato bridge, one SO_4^{2-} affording one oxygen atom and another SO_4^{2-} anion affording two oxygen atoms, forming a triple-stranded braid (Figure 1b) with a Mn···Mn separation of 3.933(9) Å. Notably, such a triple-stranded pattern of Mn^{II} formed by sulfate ions and amino acetic groups has not yet been identified thus far in metal coordination. Each triple-stranded braid is linked by the sulfate groups to two Mn^{II} ions in the neighboring braids to give a 2D framework (Figure 1c) with organic connectivity between metal centers M−L−M = 0 and inorganic connectivity = 2 (I^2O^0).[20] A polyhedral diagram is shown in Figure 1d). The nearest interchain Mn···Mn separation is 4.888(5) Å. From the topological point of view, Mn^{II} ions could be considered as 6-connected nodes linking to two carboxylate groups and four sulfate ions, which are 4-connected spacers. Thus, the overall network topology of **1** can be described as an unprecedented (4,6)-connected framework with the Schälfli symbol of (3^2;4^2;5^2)(3^4;4^4;5^4;6^3) (Figure 1e).

Magnetic Properties. Temperature dependence of the magnetic susceptibility χ_M for **1** was measured in an applied field of 1 kOe (Figure 2). The $\chi_M T$ value at 300 K is 4.23 cm^3 K mol^{-1}, close to the value expected for the noncoupled Mn^{II} ion ($S = {}^5/_2$, 4.375 cm^3 K mol^{-1}, assuming $g = 2.0$). Over the temperature range, the $\chi_M T$ value monotonously decreases but the plot of $\chi_M - T$ provides abundant information for understanding the magnetic properties of **1**. The susceptibility (χ_M) per Mn^{II} ion first increases gradually with decreasing temperature to around a maximum of 0.12 cm^3 mol^{-1} at around 12 K, then decreases rapidly until 9 K, then increases abruptly to another maximum at 5 K, and finally decreases slightly. These magnetic behaviors indicate that the magnetic properties of complex **1** are complicated. The first round maximum at around 12 K is the nature of antiferromagnetic coupling between magnetic centers, suggesting the presence of short-range antiferromagnetic ordering within the 2D plane. The second maximum at 5 K implies a possible three-dimensional magnetic ordering in complex **1** because of the antiferromagnetic coupling between layers. The reciprocal susceptibility (χ_M^{-1}) versus temperature plot above 30 K obeys the Curie−Weiss law (inset of Figure 2), with a Curie constant $C = 4.6$ cm^3 K mol^{-1} and a Weiss constant $\theta = -25.0$ K.

For a 2D system with multimode bridges, no appropriate model could be used. To estimate the coupling constant between Mn^{II} ions, the structure can be approximately regarded as a chain containing one carboxylato bridge and one mono-oxygen bridge from SO_4^{2-}. So, the magnetic behavior of **1** above 18 K can be simulated using the analytical expression derived by Fisher for a 1D Heisenberg chain of classical spins ($S = {}^5/_2$,

(19) (a) Papatriantafyllopoulou, C.; Efthymiou, C. G.; Raptopoulou, C. P.; Vicente, R.; Manessi-Zoupa, E.; Psycharis, V.; Escuer, A.; Perlepes, S. P. *J. Mol. Struct.* **2007**, *829*, 176–188. (b) Tamasi, G.; Cini, R. *Dalton Trans.* **2003**, 2928 and references cited therein.

(20) Cheetham, A. K.; Rao, C. N. R.; Feller, R. K. *Chem. Commun.* **2006**, 4780–4795.

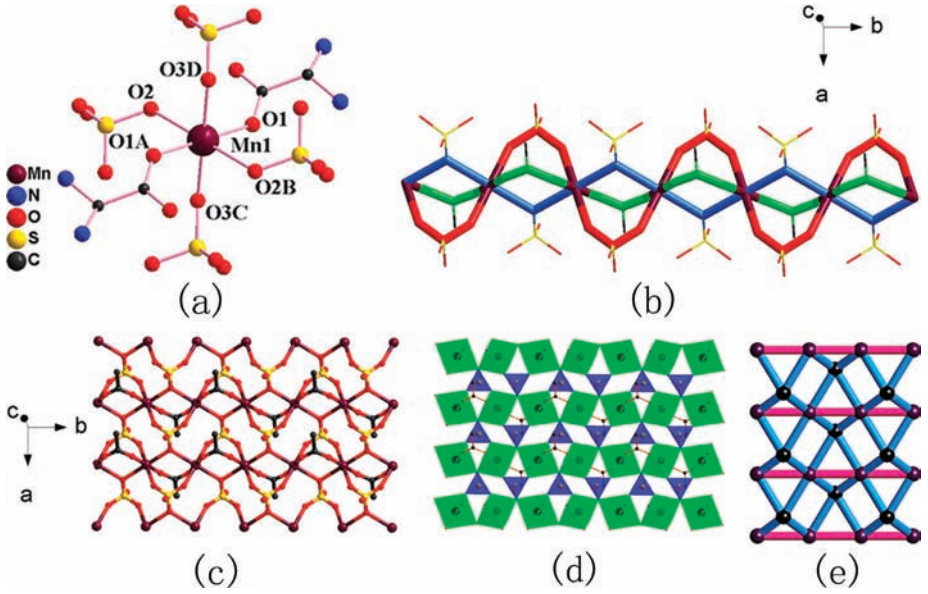

Figure 1. (a) Perspective view of the structure of the compound showing the local coordination environment of the Mn^{II} metal center, sulfate, and glycine. Hydrogen atoms are omitted for clarity. Symmetry codes: A, $-x, -y, 1-z$; B, $-x, -{}^1/_2+y, 1-z$; C, $-1-x, -y, 1-z$; D, $1+x, y, z$. (b) View of the triple-stranded braid along the b axis (red line, μ_2-SO_2 bridge; blue line, μ-SO bridge; green line, μ_2-CO_2). (c) View of the 2D structure of **1**. Amino groups are omitted for clarity. (d) Polyhedral view of the 2D structure of **1**. Green and blue polyhedra represent [MnO_6] and [SO_4], respectively. (e) (4,6) net topology of the 2D layer.

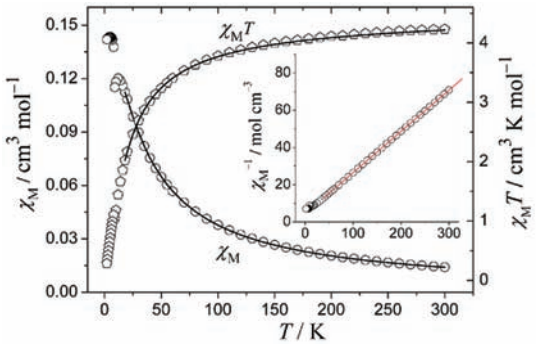

Figure 2. Temperature dependence of χ_M and $\chi_M T$ for **1**. Inset: temperature dependence of $\chi_M{}^{-1}$ for **1**. The solid line represents the best fit of the Curie−Weiss law $\chi_M = C/(T-\theta)$.

$H = -J\sum S_i \sum S_i + 1)$,[21] where J is the intrachain magnetic exchange. When the mean-field theory was used as the correcting term of the interchain interaction, the expression was described as follows:

$$\chi_{\text{chain}} = \frac{Ng^2\beta^2}{3kT}\frac{1+u}{1-u}S(S+1)$$

$$\chi_M = \frac{\chi_{\text{chain}}}{1-(2zj'/Ng^2\beta^2)\chi_{\text{chain}}}$$

where N is Avogadro's number, β the Bohr magneton, k Boltzmann's constant, $2zj'$ the interchain magnetic exchange constant, and u the Langevin function: $u = \coth[JS(S+1)/kT] - kT/[JS(S+1)]$. The best least-squares fit of the theoretical equation to experimental data leads to $J = -1.54\ \text{cm}^{-1}$, $zJ' = -0.35\ \text{cm}^{-1}$, and $g = 2.00$ with agreement factor $R = 4.76 \times 10^{-6}$ ($R = \sum(\chi_{i,\text{obsd}} - \chi_{i,\text{calcd}})^2/\sum(\chi_{i,\text{obsd}})^2$). These values indicate again the presence of a dominant weak antiferromagnetic interaction between the neighboring Mn^{II} ions in **1**. According to the structure of complex **1**, it is believed that the antiferromagnetic coupling between Mn^{II} ions is mainly mediated by the mono-oxygen bridge O2 from $SO_4{}^{2-}$. The O2 atom adopts an sp^2 hybridization and bridges to two Mn^{II} ions by the axis, so three pairs of d orbitals overlap through the O2 atom, which include $d_{z^2}(Mn)-sp^2(O)-d_{z^2}(Mn)$, $d_{xz}(Mn)-sp^2(O)-d_{xz}(Mn)$, and $d_{xz}(Mn)-p(O)-d_{xz}(Mn)$ (Figure 3). An sp^2 orbital of O2 only has a small overlap with d_{z^2} orbitals of Mn ions to form a weak σ-superexchange pathway, while d_{xz} orbitals of Mn ions partly overlap with sp^2 and p orbitals, leading to two π superexchange pathways, respectively, because they cannot be coplanar. So, all bridges mediate a weak coupling interaction between Mn^{II} ions in complex **1**.

The low-temperature magnetic behaviors of **1** suggest the presence of a weak ferromagnetic contribution below 9 K probably because of spin canting. To fully characterize the weak ferromagnetism due to spin canting, field-cooled (FC) and zero-field-cooled (ZFC) susceptibilities were performed at 10 Oe below 20 K. As shown in Figure 4, compound **1** displays weak spontaneous magnetization that can be attributed to the onset of long-range ordering of the canted spins. The divergence below 9 K indicates irreversibility of the weak ferromagnetic transition.[22] FC magnetizations at different fields (Figure 5) show a spontaneous increase below 9 K, which is more noticeable for the lower field strengths. The curves show no rise anymore at a magnetic field of 10 kOe or above, indicating that the weak antiferromagnetic interaction is overcome by the external field to result in an

(21) (a) Fisher, M. E. *Am. J. Phys.* **1964**, *32*, 343–346. (b) Kahn, O. *Molecular Magnetism*; VCH: New York, 1993.

(22) Cheng, L.; Zhang, W.-X.; Ye, B.-H.; Lin, J.-B.; Chen, X.-M. *Eur. J. Inorg. Chem.* **2007**, 2668–2676.

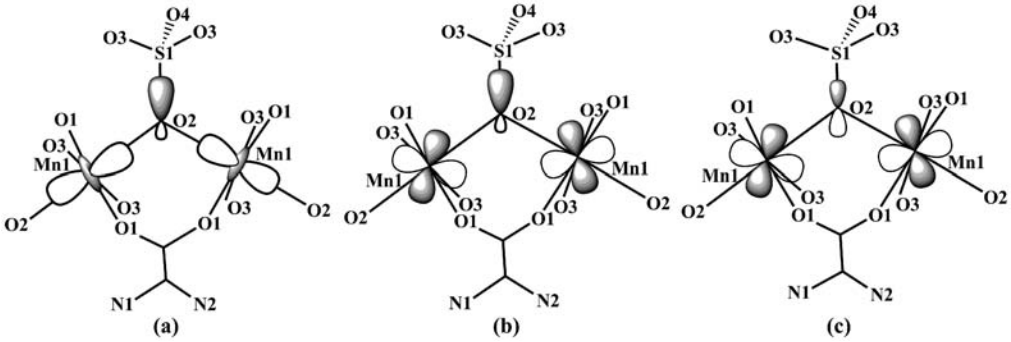

Figure 3. Schematic illustration of the overlapping orbitals: (a) $d_{z^2}(Mn)-sp^2(O)-d_{z^2}(Mn)$; (b) $d_{xz}(Mn)-sp^2(O)-d_{xz}(Mn)$; (c) $d_{xz}(Mn)-p(O)-d_{xz}(Mn)$.

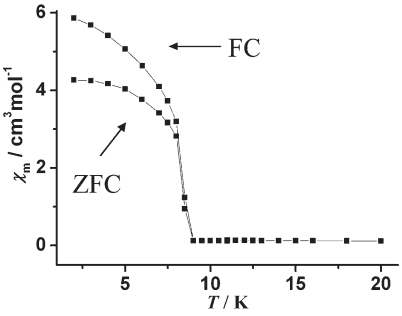

Figure 4. FC and ZFC magnetization plots at 10 Oe.

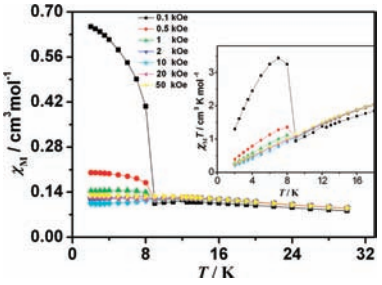

Figure 5. FC magnetizations in the form of χ_M and $\chi_M T$ (inset) vs T plots at different fields for **1**.

ordered ferromagnetic phase.[22] This field-dependent behavior of magnetic susceptibility below the critical temperature is in agreement with that of the weak ferromangets due to spin canting.[23] Further experimental evidence for the canted antiferromagnetism in **1** comes from the field-dependent isothermal magnetization $M(T,H)$ measurements at 2 K with fields up to 50 kOe (Figure 6). The magnetization increases almost linearly from 0 to 50 kOe and reaches 1.14 μ_B per Mn^{II} ion at 50 kOe, far below the saturation value $M_S = 5\ \mu_B$ for a spin-only Mn^{II} ion. In the low-field range at 2 K, a hysteresis loop can be observed with a coercivity field $H_C = 500$ Oe and a remnant magnetization $M_R = 0.011\ \mu_B$. This is consistent with the behavior of weak ferromagnetism due to spin canting.[24] The canted antiferromagnetism is also supported by the alternating-current (ac) magnetic measurements.

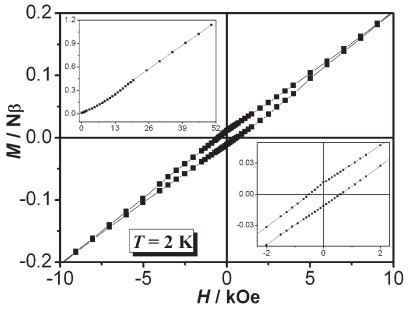

Figure 6. Hysteresis loop of **1** at 2 K. Inset: Field dependence of magnetization (left) and amplification of the loop (right).

As depicted in Figure 7, ac susceptibilities show that both in-phase (χ') and out-of-phase (χ'') signals have sharp maxima at about 9 K, and no frequency dependence was observed, which confirms further the occurrence of the magnetic transition with $T_C = 9$ K. On the basis of the results of ZFC and FC measurements, ac susceptibility measurements, and isothermal magnetization, we may safely come to the conclusion that compound **1** is a spin-canted antiferromagnet with weak ferromagnetism originating from spin canting below the critical temperature $T_C = 9$ K. The canting angle α is related to M_R and M_S through $\sin(\alpha) = M_R/M_S$[21b] and is estimated to be about 0.13°.

Usually, single-ion magnetic anisotropy and antisymmetric exchange are thought to be the two reasons for spin canting.[23a,25] Because of the isotropic character of the high-spin Mn^{II} ion, the antisymmetric exchange should be responsible for the canting in **1**. As we know, the antisymmetric exchange between a pair of spin centers vanishes when the spin centers are related by an inversion center.[23a] In the triple-stranded braid of **1**, there is no inversion center between the two adjacent Mn^{II} ions, which makes it expected that an antisymmetric exchange between the Mn^{II} ions is operative and is superimposed upon the isotropic antiferromagnetic exchange, leading to the observed spin-canting phenomenon. The spin-canting phenomenon has been well studied for the manganese complexes, most of which are bridged by azido[23a,26] or carboxylate groups.[24,27] To the best of our knowledge,

(23) (a) Yang, M.; Yu, J.; Shi, L.; Chen, P.; Li, G.; Chen, Y.; Xu, R.; Gao, S. *Chem. Mater.* **2006**, *18*, 476–481. (b) Gao, E. Q.; Yue, Y. F.; Bai, S. Q.; He, Z.; Yan, C. H. *J. Am. Chem. Soc.* **2004**, *126*, 1419–1429.
(24) Zhang, J.-Y.; Ma, Y.; Cheng, A.-L.; Yue, Q.; Sun, Q.; Gao, E.-Q. *Dalton Trans.* **2008**, 2061–2066.
(25) Armentano, D.; De Munno, G.; Lloret, F.; Palii, A. V.; Julve, M. *Inorg. Chem.* **2002**, *41*, 2007–2013.
(26) Zhang, J.-Y.; Liu, C.-M.; Zhang, D.-Q.; Gao, S.; Zhu, D.-B. *Inorg. Chem. Commun.* **2007**, *10*, 897–901.
(27) Mahata, P.; Sen, D.; Natarajan, S. *Chem. Commun.* **2008**, 1278–1280.

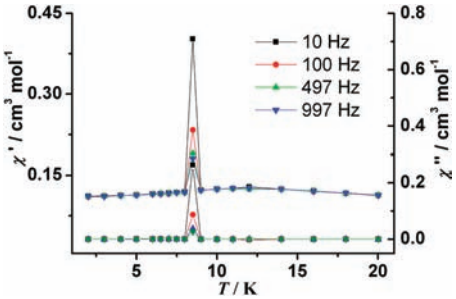

Figure 7. In-phase (χ') and out-of-phase (χ'') signals in the frequency-dependent ac magnetic susceptibility plot of **1**. Note the transition at around 9 K in both cases.

1 is the first example of a manganese polymer bridged by both sulfate ions and carboxylate groups that displays the canted antiferromagnetic behavior.

Conclusion

A novel glycine-templated sulfate material has been synthesized solvothermally. It is the first example in which the amino acid molecule has been incorporated into a transition-metal sulfate skeleton with an extended network. The compound displays a 2D framework with a novel binodal 4,6-connected ($3^2;4^2;5^2$)($3^4;4^4;5^4;6^3$) topology, which has never been reported before. The compound exhibits a spin-canted antiferromagnetic behavior with a weak ferromagnetic transition below 9 K, and the estimated canting angle is 0.13°. This work may have implications for studies on the synthesis of sulfate-based organic−inorganic or open-framework materials with novel topologies and interesting magnetic properties.

Acknowledgment. This work was supported by the National Natural Science Foundation of China (Grant 20461001), Guangxi Natural Science Foundation (Grant 0639031), and Ten-hundred-thousand Talents Program in New Century of Guangxi Province.

Supporting Information Available: The PXRD pattern, IR spectrum, TGA curve, and X-ray data file (CIF) for **1**. This material is available free of charge via the Internet at http://pubs.acs.org.